Supporting Information for the manuscript:

A Genetically Encoded AND Gate for Cell-Targeted Metabolic Labeling of Proteins

Alborz Mahdavi,[‡,*] Thomas H. Segall-Shapiro,[□,¶,§] Songzi Kou,[‡] Granton A. Jindal,[‡,^] Kevin G. Hoff,[□,†] Shirley Liu,[□] Mohsen Chitsaz,[□] Rustem F. Ismagilov,[‡] Jonathan J. Silberg,[□,¶] and David A. Tirrell[‡,*]

[‡]Division of Chemistry and Chemical Engineering, California Institute of Technology, 1200 E. California Blvd., MC 210-41, Pasadena, CA, 91125

[*]Bioengineering, California Institute of Technology, 1200 E. California Blvd., MC 210-41, Pasadena, CA, 91125

[□]Department of Biochemistry and Cell Biology, Rice University, Houston, TX 77251

[¶]Department of Bioengineering, Rice University, Houston, TX 77251

[□]Biochemistry and Molecular Biophysics, California Institute of Technology, 1200 E. California Blvd., MC 210-41, Pasadena, CA, 91125

Materials and Methods:

Creating a Library of Vectors that Express Fragmented MetRS. A *metG* fragment encoding MetRS residues 1-548 was cloned into the NcoI and SalI sites of pPROEX1 (Life Technologies) to yield pPROEX-MetRS, a vector that uses a leaky Trc promoter for expression. To make this vector compatible with library construction [1], it was digested (XbaI and SpeI) and ligated to create pPROEX-MetRSΔNotI-XS1, which lacks a NotI site. This vector was used for library construction. A NotI-flanked artificial transposon encoding chloramphenicol resistance (M1-CamR, Finnzymes) was inserted into pPROEX-MetRSΔNotI-XS1 using HyperMu, a mutant MuA transposase with increased activity (Epicentre). Reaction mixtures (20 µL) containing HyperMu buffer, 300 ng of pPROEX-MetRSΔNotI-XS1, 100 ng M1-CamR, and 1 U of HyperMu MuA transposase were incubated at 37°C for 16 h. Reactions were terminated by adding 2 µL of HyperMu 10x Stop Solution, gently mixing, and incubating each reaction at 70°C for 10 min. Total DNA was purified (Zymo Research) and electroporated into *E. coli* MegaX DH10B. Colonies (~180,000) appearing after 24 h on selective medium (20 µg/mL chloramphenicol) were harvested from plates and pooled, and total plasmid DNA was purified using a Qiagen Miniprep Kit to obtain a library of vectors encoding MetRS genes with a transposon (M1-CamR) inserted at different locations. This library was digested with restriction enzymes (BspHI, ClaI, and NdeI) that cut at two sites within *metG* (base pairs 73-78 and 1603-8) and five sites within the pPROEX vector. MetRS genes (base pairs 73-1608) containing M1-CamR were separated from other DNA fragments by agarose gel electrophoresis, purified, and cloned back into pPROEX-MetRSΔNotI-XS1. These vectors containing size-selected MetRS genes were electroporated into *E. coli* MegaX DH10B, colonies (~118,000) appearing on LB-agar plates containing 20 µg/mL chloramphenicol were harvested, and total DNA was purified to obtain a size-selected library. The M1-CamR was removed from the size-selected library by NotI digestion and replaced with *f1-kan*^{R}, a DNA insert that terminates translation preceding the insert and initiates transcription and translation following the insert [1]. The resulting two-promoter library was electroporated into *E. coli* MegaX DH10B, plated onto LB-agar medium containing 25 µg/mL kanamycin and incubated for 24 h at 37°C. Colonies (~248,000) were harvested, and total DNA was purified to obtain the two-promoter library used for functional selections.

An *E. coli* Selection for Functional MetRS. The λDE3 Lysogenization Kit (Novagen) was used to generate DE3 lysogens of *E. coli* CS50 (Yale Stock Center), a strain that grows slowly in the absence of methionine because of a MetRS mutation that increases the K_M for Met [2]. To identify a CS50-DE3 lysogen that constitutively expresses T7 RNA polymerase, cells were transformed with pET-Venus-Grx2[3] and their fluorescence was measured using a Tecan M1000 plate reader. An *E. coli* CS50-DE3 strain from this

screen was electroporated with the final two-promoter library, plated on M9 minimal media containing all amino acids except methionine, and grown for 24 hours at 37°C. Vectors from one hundred colonies were picked and used to inoculate LB cultures containing 50 μg/mL ampicillin. DNA purified from each overnight culture was sequenced.

Evaluation of MetRS Complementation Strength. After sequencing, complementing vectors were transformed into *E. coli* CS50-DE3, plated onto LB-agar plates containing 50 μg/mL ampicillin, and incubated at 37°C for 24 h to obtain colonies. Overnight LB cultures from three separate colonies of each variant were diluted to OD_{600} = 2.0, 0.2, 0.02, and 0.002, and 10 μL of each was spotted onto +Met and –Met M9-agar plates. Prior to spotting, cells were harvested by centrifugation, washed three times with 25% glycerol, and resuspended in 25% glycerol to OD_{600} = 2. Growth was visually assessed after 24 h, when cells harboring pPROEX showed no visible growth and cells containing pPROEX-MetRSΔNotI-XS1 grew at all titers. Cell growth was scored on a scale of 1 to 4, based on the number of dilutions where growth was visible. MetRS-NLL did not complement *E. coli* CS50-DE3 growth after 24 h, and thus could not be used as a parent for laboratory evolution experiments.

Calculation of Residue-Residue Contacts in Each Split Variant. The number of intermolecular contacts made between fragments of all possible split MetRS variants was calculated as the number of residue pairs with atoms within a distance cutoff of 4.5 Å. Protein Data Bank crystal structure 1f4I was used for this analysis [4].

Introduction of Active Site Mutations into Selected MetRS Vectors. Site-directed mutagenesis (Stratagene) was used to mutate MetRS residues L13, Y260 and H301 to PLL (or NLL) in seven complementing vectors selected from the two-promoter library (pPROEX-MetRSΔNotI-XS1 derived), including variants 48, 131, 183, 247, 272, 278 and 456 (see Fig. S3). Split proteins with mutations are designated NLL-MetRS(cut site) and PLL-MetRS(cut site), respectively.

Vectors for Regulated Protein Expression. A fragment of the MetRS gene encoding NLL-MetRS residues 1-247 was cloned into pQE80L-Kan between the BamH1 and Sal1 restriction sites to create pQE80His6_N247. This vector drives expression of the N-terminal MetRS fragment with an N-terminal His_6-tag under control of an IPTG-inducible T5 promoter. A fragment of the MetRS gene encoding NLL-MetRS residues 247-548 was cloned into pBAD33 between the Sac1 and Kpn1 restriction sites to create pBAD33HA_C247. This vector drives expression of the C-terminal MetRS fragment with a C-terminal hemagglutinin tag (YPYDVPDYA) under control of an arabinose-inducible and glucose-repressible P_{BAD} promoter. Translational initiation on pBAD33-derived mRNAs was accomplished by introducing before

the ATG start codon a DNA sequence (AGGAGGAATTCACC) that encodes a ribosome-binding site. Vectors for assessing promoter activities in gradients of inducers were generated by cloning GFP into pBAD33 and pQE80L-Kan to create pQE80L-GFP and pBAD33-GFP, respectively.

Synthesis of Azidonorleucine. Azidonorleucine synthesis was based on a previous protocol for synthesis of azidohomoalanine, using Boc-lysine as the starting material [5]. Briefly, 5.27 g (81.1 mmol) of sodium azide was treated with 2.7 mL (16 mmol) of distilled triflic anhydride in 13 mL of water for 2 h. The triflic azide product was extracted with 10 mL methylene chloride and added dropwise to a flask containing Boc-Lys-OH (2 g, 8.1 mmol), K_2CO_3 (1.68 g, 12.2 mmol) and $CuSO_4$ (20 mg, 0.08 mmol) in 26 mL of water and 250 mL of methanol. After 20 h at room temperature the product was extracted with ethyl acetate, redissolved in methylene chloride and purified by silica gel chromatography. After Boc deprotection with hydrochloric acid, the final product was purified by cation exchange chromatography.

Metabolic Incorporation of Anl into Cells Grown in Liquid Culture. To test metabolic incorporation of Anl into proteins in *E. coli* cells expressing split MetRS variants, overnight LB cultures were used to inoculate cultures containing M9 minimal media containing 19 amino acids (100 µM), 100 µM methionine, and 1% glycerol. Cells were grown in minimal media to an OD_{600} = 0.25, Anl was added at a final concentration of 1 mM, and cells were grown for 1 h to allow for metabolic incorporation of Anl into newly synthesized proteins. For experiments involving cells transformed with pairs of inducible vectors (*e.g.*, pQE80His6_N247 and pBAD33HA_C247), cells were grown to an OD_{600} = 0.25, arabinose and IPTG inducers were added at varying concentrations, cells were grown for 2 h, Anl was added at a final concentration of 1 mM, and cells were grown for 1 h to allow for metabolic incorporation of Anl into newly synthesized proteins. For AND-gate expression, based on the two vector system (pQE80His6_N247, pBAD33HA_C247), 50 µg/ml of kanamycin and 100 µg/ml of chloramphenicol were used. Cells were harvested by centrifugation at 10,000 rcf for 5 minutes and lysed with 4% SDS (10 µL for cell pellets resulting from 1 mL of culture medium) prior to labeling of the lysate with alkyne-TAMRA dye (structure **2**, Fig. 2E).

Labeling Anl-tagged Proteins in Cell Lysates with an Alkyne-TAMRA Dye. Cells were lysed with 4% SDS in phosphate buffered saline (PBS). Ethylenediaminetetraacetic acid (EDTA)-free protease inhibitor (Roche) was added to the lysates to reduce protease activity. The EDTA-free version of the protease inhibitor was required for copper-catalyzed cycloaddition reactions because EDTA chelates copper ions and interferes with copper-dependent reactions. PBS was added to dilute the SDS concentration to 1%, and cell lysates were centrifuged at 14,000 rcf for 10 min to remove cellular debris. Protein concentrations were measured by using a bicinchoninic protein quantification kit (BCA assay; Pierce,

Rockford, IL). The same amount of protein was used for each condition; concentrations ranged from 0.1 to 0.4 mg/mL. Copper-catalyzed reactions were performed at room temperature for 2 h in 1.5 mL centrifuge tubes, according to the following protocol: (i) alkyne-TAMRA dye was added to protein solution to a final concentration of 100 µM; (ii) tris(3-hydroxypropyltriazolylmethyl)amine (THPTA) and copper sulfate were pre-incubated together for 1 min and then added to the protein solution to final concentrations of 0.1 mM copper sulfate and 0.5 mM THPTA; (iii) aminoguanidine was added followed by sodium ascorbate (made fresh in water), and (iv) the solution was mixed once and protected from light with no further mixing. The final concentrations of aminoguanidine and sodium ascorbate were 5 mM. The THPTA ligand was synthesized according to methods published by Finn and coworkers [6]. Proteins were precipitated with chloroform/methanol, washed with methanol to remove unreacted dye and resuspended in protein loading buffer containing 2% SDS and 10% mM 2-mercaptoethanol. Proteins were electrophoresed using 12% Bis-Tris polyacrylamide gels (Invitrogen). TAMRA ($\lambda_{excitation}$ = 555 nm and $\lambda_{emission}$ = 580 nm) was excited at 532 nm and detected with a 580 band-pass 30 nm filter. In-gel fluorescence images were acquired on a Typhoon 9400 instrument (GE Healthcare).

Copper-free Protein Labeling with Dibenzocyclooctyne-TAMRA. Cells were lysed with reducing buffer containing 5 mM dithiothreitol, 4% SDS in PBS and incubated for 30 min at 50ºC. The SDS concentration was then reduced to 1% by addition of PBS. The lysates were subsequently incubated in the dark for 30 min with 100 mM iodoacetamide. The reduction and alkylation steps were used to reduce background labeling due to reaction with free thiols. After reduction and alkylation, the proteins were reacted with 20 µM azadibenzocyclooctyne-TAMRA dye conjugate (Click Chemistry Tools, AZ) for 15 min at room temperature, precipitated with chloroform/methanol and washed with methanol to remove unreacted dye.

Western Blot Detection of Split-MetRS Fragment Expression. N-terminal fragments expressed from pQE80His6_N247 contained N-terminal His_6 tags. These fragments were detected by western blot analysis using an AlexaFluor 488 conjugated anti-penta-His antibody (Qiagen). AlexaFluor 488 ($\lambda_{excitation}$ = 495 nm and $\lambda_{emission}$ = 520 nm) was excited at 488 nm and detected with a 520 band-pass 40 nm filter. C-terminal fragments expressed from pBAD33HA_C247 contained C-terminal hemagglutinin (HA) tags. HA-tagged proteins were detected by western blot analysis with AlexaFluor 633 conjugated anti-HA antibody (Santa Cruz). AlexaFluor 633 ($\lambda_{excitation}$ = 632 nm and $\lambda_{emission}$ = 647 nm) was excited at 633 nm and detected with a 670 band pass 30 nm filter. All images were obtained on a Typhoon 9400 instrument (GE Healthcare).

Fabrication of the Microfluidic Laminar Flow Device. The microfluidic device was fabricated using rapid prototyping in polydimethylsiloxane (PDMS) [7]. The channel geometry is shown in Fig. S8. Inlet channel widths were 850 μm; the main channel width was 870 μm. The channel depth was 175 μm. The PDMS mold was plasma oxidized and attached to a 0.17 mm thick glass slide. The attached PDMS mold and glass slide were heat cured at 110°C for 10 min. To render the glass surface and channel surface cell-adhesive, the device was filled with 1 mg/mL Poly-D-lysine (Millipore, MA) in PBS and then dried for 12 h at 37°C [8].

Modeling Diffusion in the Microfluidic Channel. The channel geometry was constructed in AutoCad 2012 (Autodesk Student version) software and diffusion simulations were performed using COMSOL® Multiphysics v4.2a with the Laminar Flow module and Transport of Diluted Species module. A mesh with a maximum element size of 25 μm was used for this analysis. For these simulations, we used a flow rate of 1 μL/min and inlet concentrations of arabinose and IPTG of 5 mM and 1 mM, respectively. The diffusion coefficients of arabinose and IPTG were estimated using the Stokes-Einstein equation according to the diffusion coefficient of glucose in water at 37 ºC, which is 9.59 $\times 10^{-10}$ $m^2 \cdot s^{-1}$ [9]. The estimated values we used here were 1.02×10^{-9} $m^2 \cdot s^{-1}$ for arabinose and 8.74×10^{-10} $m^2 \cdot s^{-1}$ for IPTG. These values are in agreement with previously reported diffusion coefficients of arabinose [10] and IPTG [11] at 37 ^{o}C. See Fig. S8-S9 for further details.

Imaging Dye Diffusion in the Microfluidic Channel. Dye diffusion experiments were performed to measure dye profiles in the channel and compare the measured and predicted profiles. One inlet contained a solution of AlexaFluor488 dye at a concentration of 2.82 μM; the second inlet contained PBS. Fluorescence images were obtained with a Leica DMI6000 microscope (Leica, CT) with a 10× (0.40 N.A.) objective, which was coupled to a cooled-CCD camera with 12-bit, 1344×1024 resolution (Hamamatsu Photonics, UK) and a 0.6× coupler. The filter cube (Leica) had excitation range: BP 480/40; dichromatic mirror: 505; suppression filter: BP527/30. Images were obtained at the solid-liquid interface on the glass surface of the channel. Imaging the dye diffusion at the glass-liquid interface was done as a surrogate for the PDMS-liquid interface on which the cells are seeded, to reduce effects from bulk fluorescence of the dye.

Cell Seeding and Induction in the Microfluidic Channel. Overnight LB cultures were inoculated into M9 minimal media containing 19 amino acids (100 μM), 100 μM Met, and 1% glycerol, and incubated at 37^{o}C until they reached an OD_{600} = 0.4. The cells were seeded on the PDMS surface of the microfluidic channel for 2 h at 30°C with no fluid flow. The micro-channel was flushed with M9 minimal medium containing 0.5 mg/mL glucose. Cells were incubated in this medium at 37°C for 30 min prior to

induction, with no flow. M9 minimal media containing 1 mM Anl and one of the two inducers (1 mM IPTG or 5 mM arabinose) were loaded into two different 250 µL gas-tight Hamilton syringes (Hamilton Company, MA), and the two converging laminar streams were pumped through the device. Flow rates were controlled using syringe pumps (Harvard Apparatus, MA); a flow rate of 1 µL/min was used for each stream. Inductions were performed for 4 h. After induction, inducer solutions were flushed from the channel with PBS, and cells were fixed with 3.7% formaldehyde at 37°C for 15 min and washed for 10 min with PBS. Cells expressing GFP were imaged in PBS, whereas cells expressing the split MetRS were permeabilized with methanol for 3 min, washed with PBS for 10 min, and treated with alkyne-AlexaFluor 488 dye prior to imaging (under the same conditions described above for labeling of lysates with alkyne-TAMRA dye). The dye was washed out of the channel for 1 h with PBS (2 µL/min) before fluorescence imaging.

Fluorescence Imaging of Cells in the Microfluidic Channel. Fluorescence and bright field images were obtained with a Leica DMI6000 microscope (Leica, CT). We used a 10× (0.40 N.A.) objective, which was coupled with a cooled CCD camera with 12-bit, 1344×1024 resolution (Hamamatsu Photonics, UK) with a 0.6× coupler. MetaMorph Imaging software (version 7.7) was used for image acquisition. The filter cube (Leica) used for GFP was L5 (Excitation range: BP 480/40; Dichromatic mirror: 505; Suppression filter: BP527/30), the same filter set was used for imaging alkyne-AlexaFluor 488 dye.

Quantification of Fluorescence in the Microfluidic Channel. Fluorescence images of the cells in the microfluidic channel were analyzed using ImageJ software. For quantification of fluorescence, the width of the channel was divided into 17 equally spaced boxes (as shown in Fig. 4*C*), starting 50 µm from each wall to avoid edge effects. Each box was 45 µm in height and 420 µm in length; a picture of one box located 50 µm from the edge is shown in Fig. 4*C*. The mean fluorescence intensity in each box was measured. This measurement was performed at three adjacent locations, with the upstream edge of the first box located 2 mm downstream from the y-junction of the channel, and adjacent boxes placed immediately downstream. Fluorescence measurements were used to calculate the mean and standard deviation at each position across the width of the channel. Fluorescence intensities are reported relative to the highest value.

Fluorescence Confocal Images of Labeled Proteins in Cells. Fluorescence confocal images were not obtained directly from the microfluidic channel due to the thickness of the glass slide. Overnight LB cultures were inoculated using the same method used for seeding in the microfluidic channel. Cells were seeded into a 6-well chamber slide (Lab-Tek, Thermo Fischer Scientific), and induction was performed according to the method used for the microfluidic channel. After induction, cells were fixed with 3.7%

formaldehyde at 37°C for 15 min and washed three times with PBS. Cells were permeabilized with methanol for 3 min and washed three times with PBS. The copper-catalyzed dye-labeling reaction was performed (according to the conditions described for labeling of lysates with alkyne-TAMRA dye above) using alkyne-AlexaFluor 488 dye. The reaction volume was 200 µL per well. After dye-labeling for 2 h, the cells were washed with five sequential PBS washes of 300 µL each, over a period of 2 h. The chamber slide was removed from the glass slide, and the cells were covered with 10% glycerol in PBS under a coverslip. Imaging of AlexaFluor 488 fluorescence was performed on a Zeiss LSM 510 microscope using excitation and emission wavelengths of 495 nm and 519 nm, respectively.

Table S1. Functional MetRS variants discovered using *E. coli* CS50-DE3 complementation. For each variant, we indicate: (i) the MetRS residues produced by the first open reading frame, ORF1, (ii), the relative orientations of the promoters preceding and within *metG*[1], (iii) if open reading frame following the internal promoter is in frame, (iv) the MetRS residues predicted to be produced by ORF2 following the internal promoter, (v) the relative complementation strength of each variant scored on a scale of 1-4, and (vi) the number of occurrences of each unique variant within the sequenced clones. In cases where ORF2 is out of frame, the MetRS residues present in the second fragment are unknown and the initial residue is designated alternative (alt) start codon. In the clone where the promoters are anti-parallel, ORF2 is not translated or transcribed.

ORF1 (residues)	Promoter orientations	ORF2 in frame	ORF2 (residues)	Relative Activity	Number clones
1-31	parallel	no	alt-548	3	1
1-40	parallel	no	alt-548	2	1
1-43	parallel	yes	43-548	2	1
1-48	parallel	yes	48-548	2	1
1-52	parallel	no	alt-548	2	1
1-55	parallel	yes	55-548	3	1
1-114	parallel	no	alt-548	2	1
1-131	parallel	yes	131-548	3	1
1-138	parallel	no	alt-548	2	1
1-152	parallel	no	alt-548	2	1
1-183	parallel	no	alt-548	2	1
1-183	parallel	yes	183-548	3	2
1-221	parallel	no	alt-548	2	1
1-247	parallel	yes	247-548	4	46
1-272	parallel	yes	272-548	3	1
1-273	parallel	no	alt-548	1	2
1-274	parallel	yes	274-548	3	1
1-278	parallel	yes	278-548	3	2
1-294	parallel	yes	294-548	1	1
1-373	parallel	no	alt-548	2	1
1-393	parallel	yes	393-548	2	1
1-416	parallel	no	alt-548	2	1
1-454	parallel	no	alt-548	2	1
1-456	parallel	yes	456-548	2	1
1-494	parallel	yes	494-548	2	1
1-534	parallel	no	alt-548	2	1
1-538	anti-parallel	---	---	3	2

Figure S1. Complementation of *E. coli* CS50-DE3 by selected MetRS variants. Growth after 24 hours at 37°C of *E. coli* CS50-DE3 transformed with: i) pPRO-EX, ii) pPROEX-MetRSΔNotI-XS1, and pPRO-EX vectors that express fragmented MetRS variants discovered in selections. After sequencing, each vector was transformed into CS50-DE3 to obtain individual colonies on LB-agar plates, and the complementation of three separate colonies was analyzed on minimal medium containing or lacking methionine. Serial dilutions (1x, 10x, 100x, and 1000x) of the resuspended cells (10 µL each) were spotted in triplicate onto two M9-agar plates. NLL-MetRS did not complement *E. coli* CS50 in the absence of methionine.

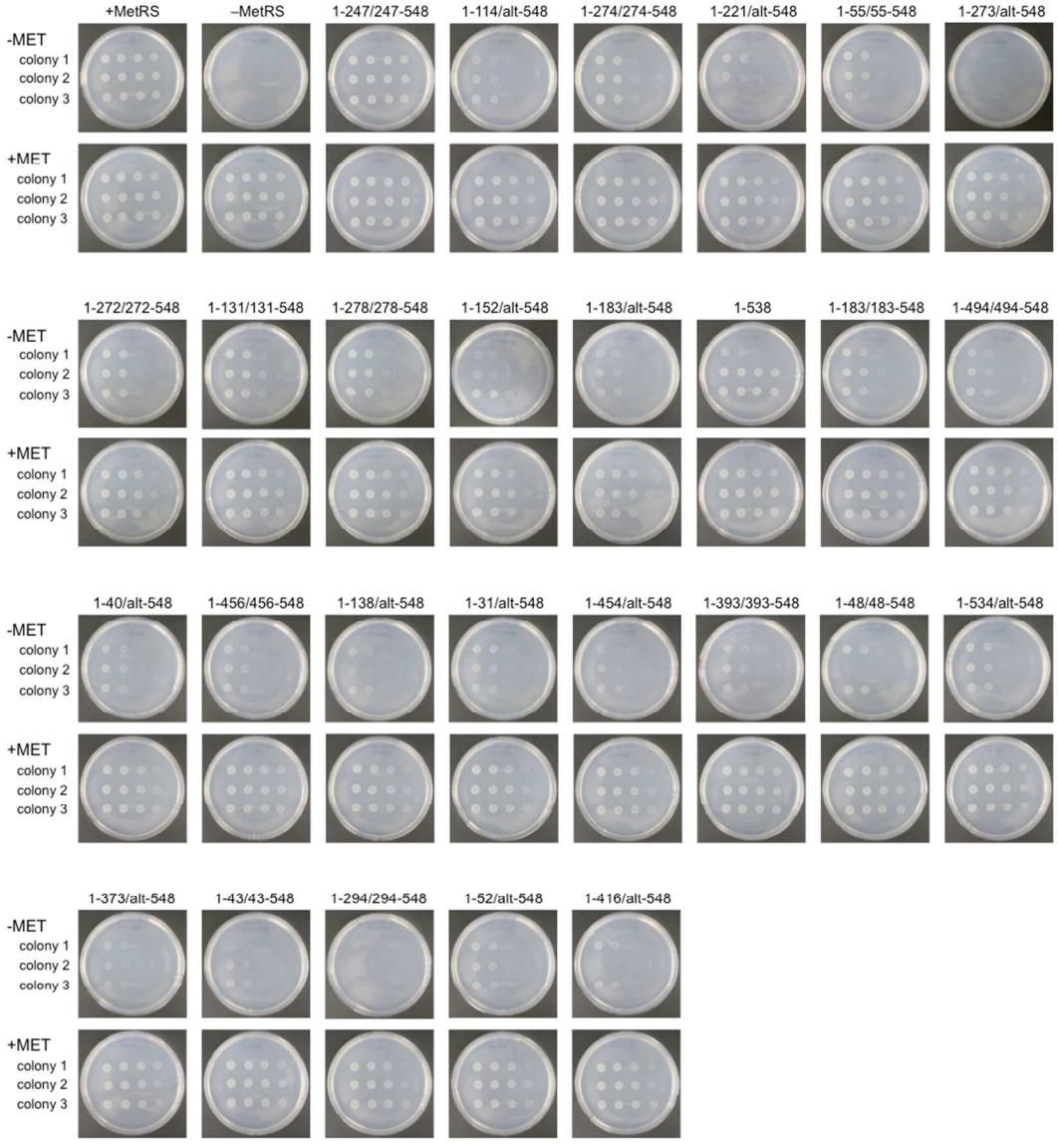

Figure S2. Intermolecular contacts between fragments. The number of intermolecular interactions between fragments in each split MetRS variant was calculated by counting the number of residue–residue contacts across the inter-fragment interface. Residues were considered interacting if any of their atoms were within 4.5 Å of one another. Calculations are based on the MetRS crystal structure (Protein Data Bank code 1f4l) [4].

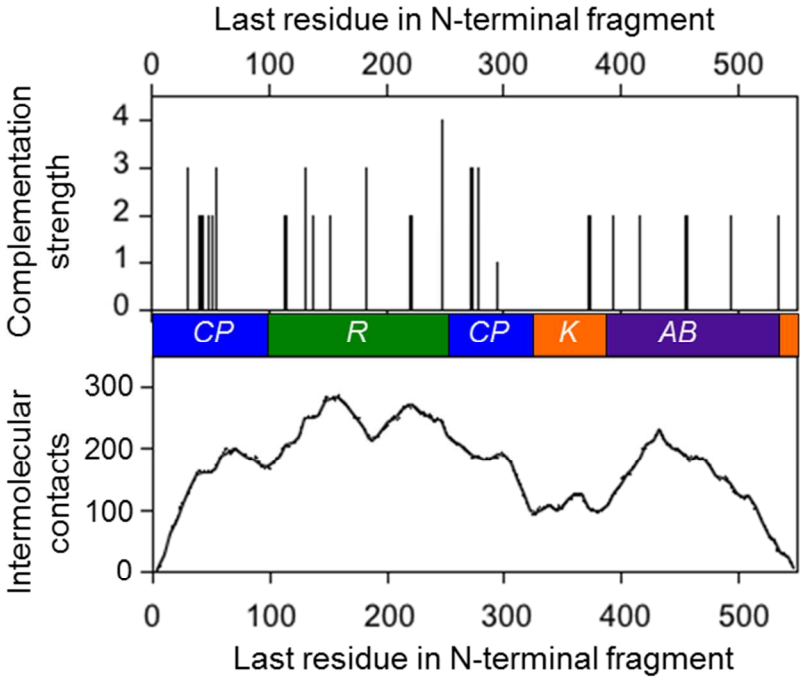

Figure S3. Structural models for fragmented MetRS variants. PDB structure 2CSX[12] was used to generate structural models for the seven split MetRS variants that were screened for Anl labeling activity after mutation of residues L13, Y260 and H301 to NLL and PLL, respectively. These variants were chosen because they were among the most active fragmented MetRS in bacterial complementation measurements. The backbone cleavage sites were distributed through different domains of the protein in these variants. For each variant, residues in the N-terminal MetRS fragment are shown in blue, residues from the C-terminal fragment are shown in magenta, and bound tRNA is shown in orange. Split MetRS are named based on the last residue within the N-terminal fragment before peptide backbone cleavage, *e.g.,* MetRS(247). This residue is duplicated and found in both the N-terminal and C-terminal fragments in our constructs generated by transposase mutagenesis [1].

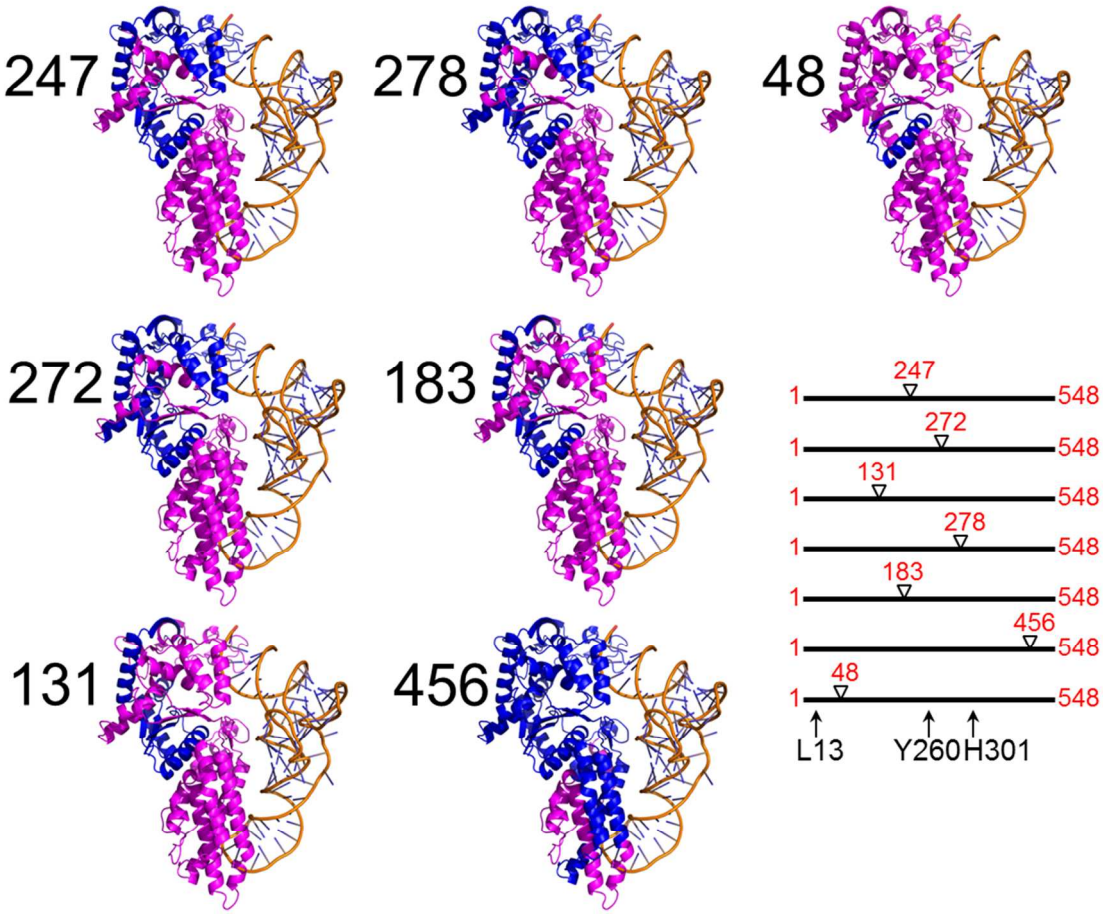

Figure S4. Anl labeling in cells expressing NLL-MetRS(247) under control of regulated promoters. *E. coli* DH10B cells transformed with vectors encoding NLL-MetRS(247) [pQE80His6_N247 and pBAD33HA_C247] were grown in M9 minimal media containing 19 amino acids, 100 µM methionine, and 1% glycerol. At OD_{600} = 0.25, IPTG and arabinose were added to final concentrations of 1 mM and 5 mM, respectively. Cells were grown for 2 h after induction, Anl was added to a final concentration of 1 mM, and cells were grown for an additional 1 h to allow for Anl incorporation into newly synthesized proteins. Cells were lysed, and lysates were treated with a TAMRA-alkyne dye. Proteins from the cell lysate were separated by SDS-PAGE, and TAMRA-labeled proteins were detected by in-gel fluorescence imaging.

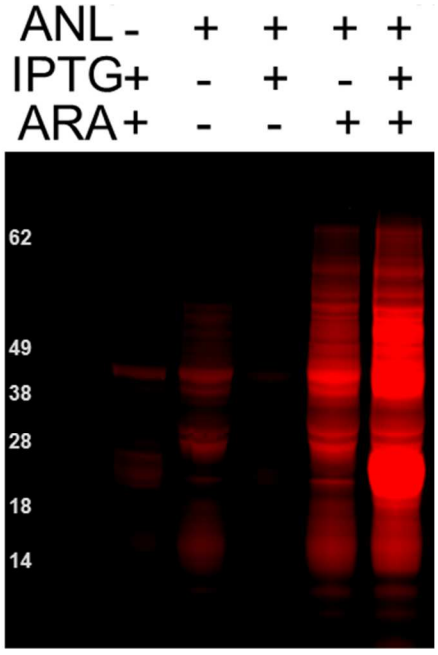

Figure S5. Effect of glucose on NLL-MetRS(247) activity. *E. coli* DH10B cells transformed with vectors encoding NLL-MetRS(247) [pQE80His6_N247 and pBAD33HA_C247] were grown in M9 minimal media containing 19 amino acids, 100 µM methionine, 1% glycerol, and varying glucose concentrations (0, 0.1, 0.5, 1, 5 mg/ml). At OD_{600} = 0.25, IPTG and arabinose were added to final concentrations of 1 mM and 5 mM, respectively. Cells were grown for 2 h after induction, Anl was added to a final concentration of 1 mM, and cells were grown for 1 h to allow Anl incorporation into newly synthesized proteins. Cells were lysed and lysates were treated with a TAMRA-alkyne dye. Proteins from the cell lysate were separated by SDS-PAGE and Anl-labeled proteins were detected by in-gel fluorescence imaging. Colloidal blue staining of the same gel shows similar protein levels in each lane. Labeling observed under similar conditions with cells expressing intact NLL-MetRS under control of its endogenous MetG promoter in pQE80[13] is shown for comparison.

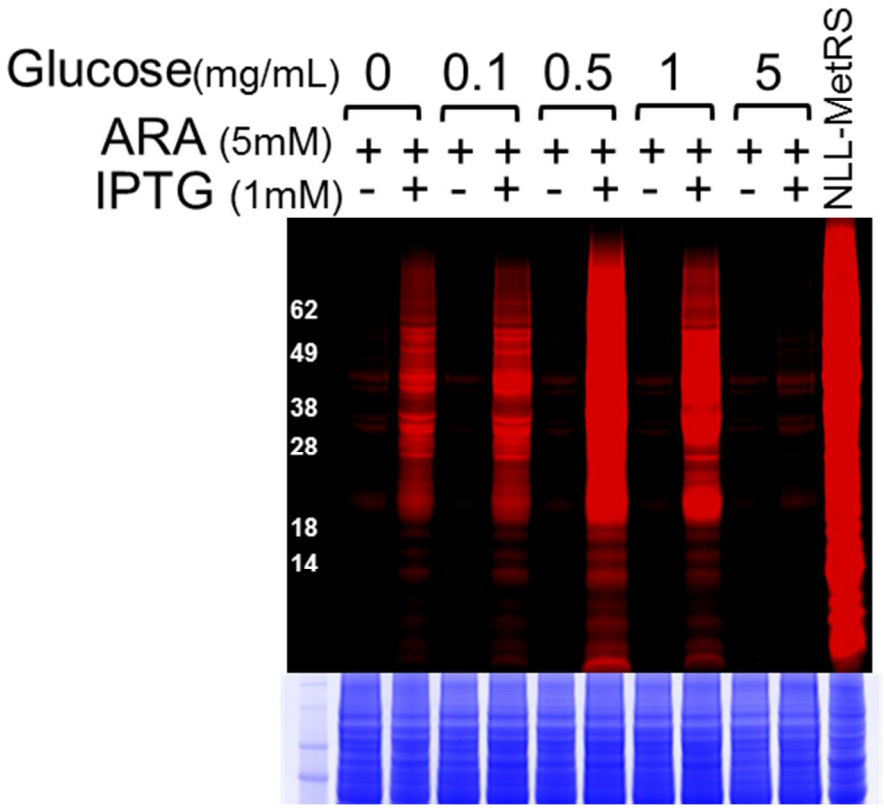

Figure S6. Effect of varying IPTG and arabinose concentrations on NLL-MetRS(247) activity. *E. coli* DH10B cells transformed with vectors encoding NLL-MetRS(247) [pQE80His6_N247 and pBAD33HA_C247] were grown in M9 minimal media containing 19 amino acids, 100 µM methionine, 1% glycerol, and 0.5 mg/mL glucose. At OD_{600} = 0.25, 25 different concentrations of arabinose and IPTG were added to cultures. IPTG was added to final concentrations of 0 µM, 10 µM, 100 µM, 1 mM and 5 mM. Arabinose was added to final concentrations of 0 mM, 0.1 mM, 1 mM, 6.7 mM and 12 mM. Cells were grown for 2 h after induction, Anl was added to a final concentration of 1 mM, and cells were grown for 1 h to allow Anl incorporation into newly synthesized proteins. Cells were lysed and lysates were treated with a TAMRA-alkyne dye. Proteins from the cell lysate were separated by SDS-PAGE, and Anl-labeled proteins were detected by in-gel fluorescence imaging (top panel). The bottom gel shows a Western blot of the cell lysates using an AlexaFluor488-conjugated anti penta-His antibody that detects the N-terminal MetRS fragment (green) and an AlexaFluor647-conjugated anti hemagglutinin antibody that detects the C-terminal MetRS fragment (blue).

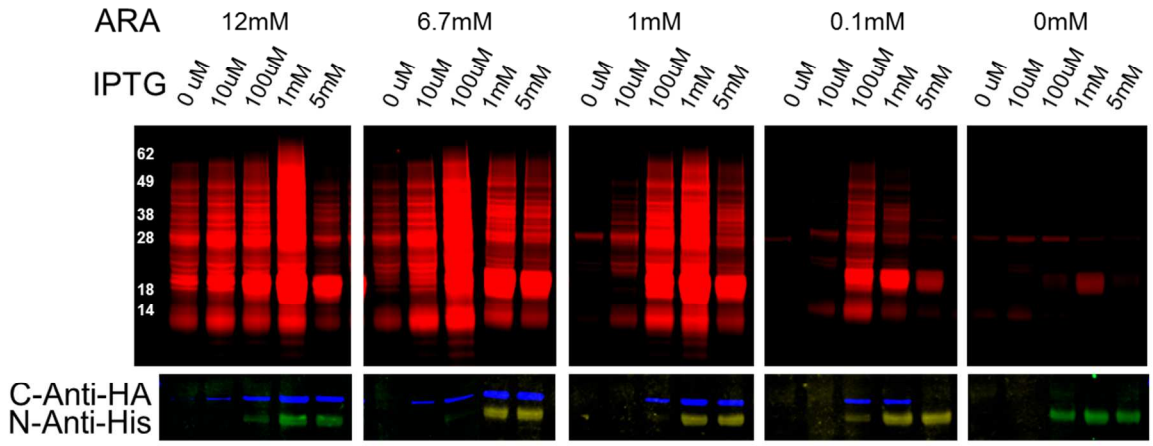

Figure S7. Kinetics of AND-gate activation and protein labeling. (**a**) Kinetics of AND gate activation: *E. coli* DH10B cells transformed with vectors encoding NLL-MetRS(247) [pQE80His6_N247 and pBAD33HA_C247] were grown in M9 minimal medium containing 19 amino acids, 100 µM methionine, 1% glycerol, and 0.5 mg/mL glucose. The N- and C-terminal fragments were induced by addition of IPTG and arabinose at 1 mM and 5 mM, respectively. Anl was added at 1 mM at the time of induction. As a control for background labeling, cells were also incubated in 1 mM Anl without IPTG and arabinose for 200 min. After Anl incorporation for various times (0 – 180 min), cells were lysed and treated with azadibenzocyclooctyne-TAMRA dye (see supplementary methods). TAMRA labeling (top left) indicating Anl incorporation was detected by in-gel fluorescence imaging. Colloidal blue labeling of the same gel (bottom left) was used to compare protein loading across lanes. Quantification of Anl incorporation was done by measuring TAMRA fluorescence at three different bands in each lane and dividing these values by the band intensities from colloidal blue labeling, thereby normalizing for differences in protein amounts between different conditions. The level of Anl labeling in the absence of IPTG and arabinose was also measured after 200 min, and is represented by the red dot in the mean-normalized TAMRA fluorescence intensity plot.

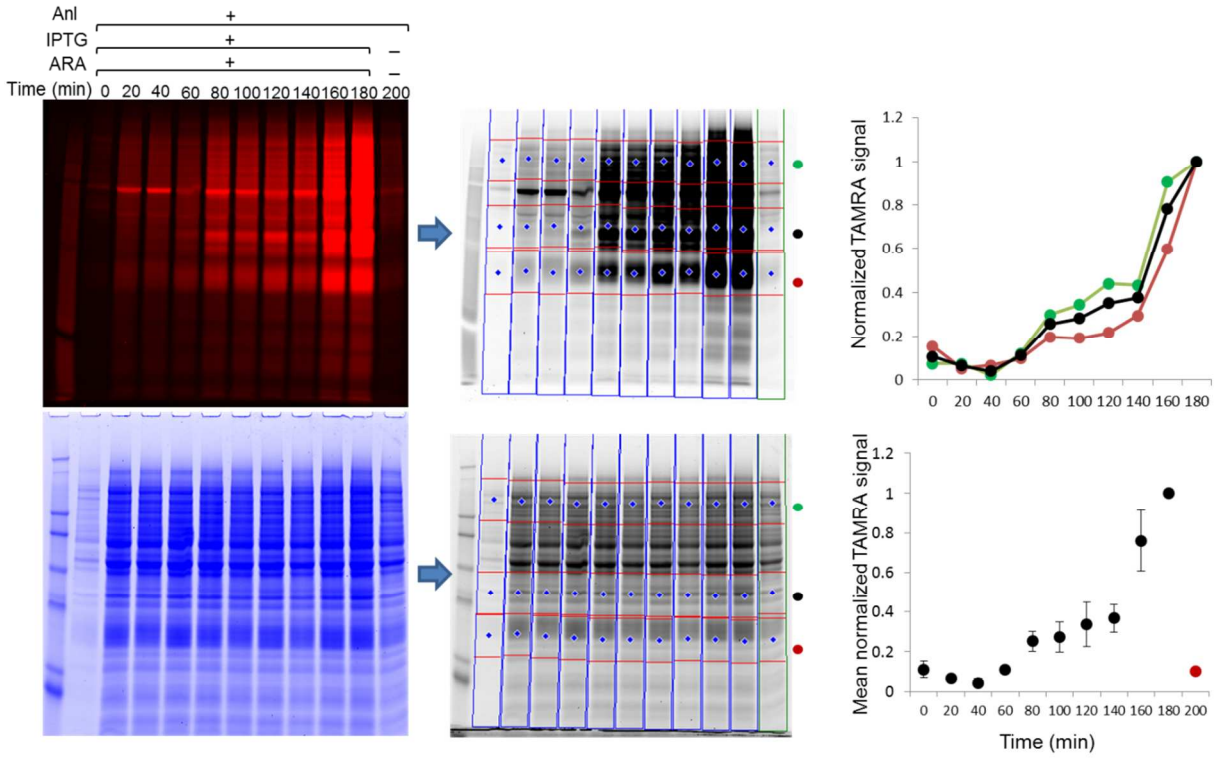

(**b**) Kinetics of Anl incorporation under control of the activated AND gate: Cells transformed with vectors encoding NLL-MetRS(247) [pQE80His6_N247 and pBAD33HA_C247] were grown in M9 minimal media containing 19 amino acids, 100 µM methionine, 1% glycerol, and 0.5 mg/mL glucose. The N- and C-terminal fragments were induced by addition of IPTG and arabinose at 1 mM and 5 mM, respectively, for 3 h. Anl was then added at 1 mM. Under these conditions, fragment expression is not the rate-limiting step for Anl incorporation. As a control for background labeling, cells were also incubated in 1 mM Anl without IPTG and arabinose for 65 min; the TAMRA signal for this control is shown by red symbol in the quantification results. Quantification was performed as described above.

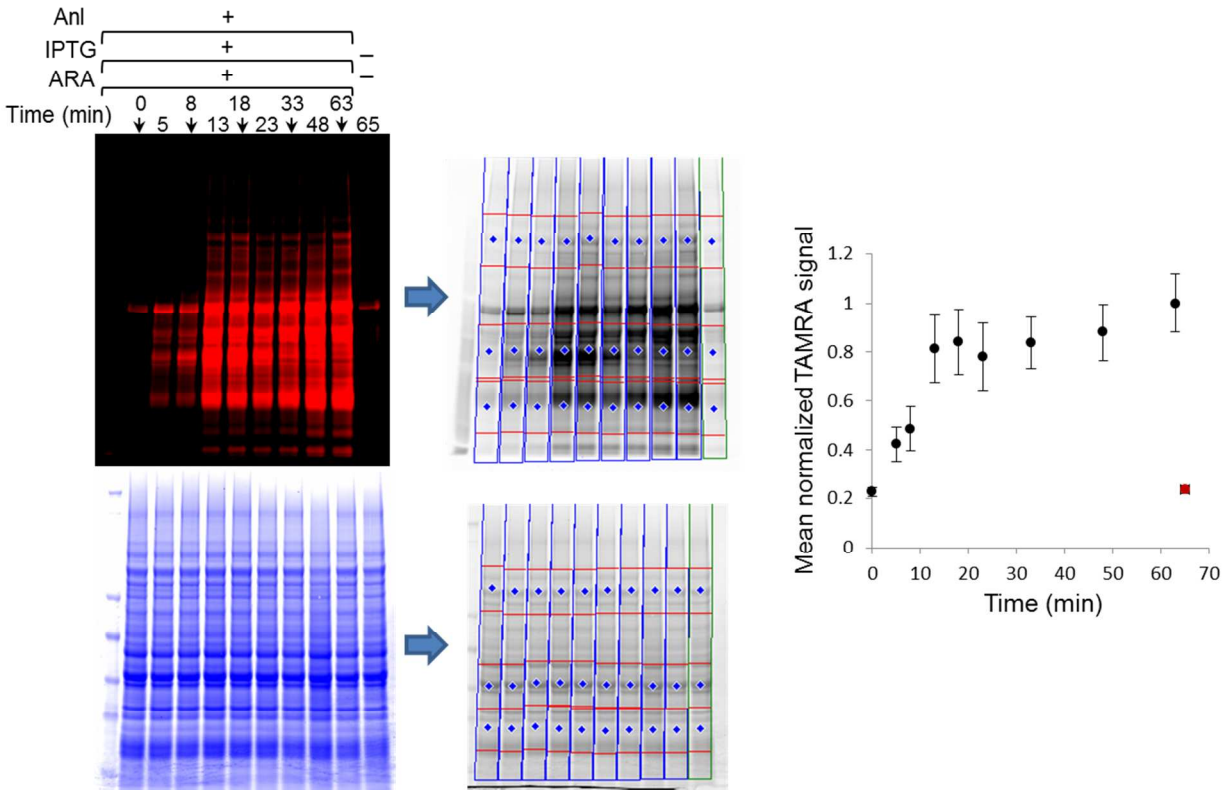

Figure S8. Modeling the diffusion of IPTG and arabinose in the microfluidic channel.

To determine the profiles of IPTG and arabinose in the microfluidic channel, the dimensions of the channel shown in (*A*) were entered into AutoCad software and imported into Comsol software to model diffusion at the liquid-liquid interface. A flow rate of 1 µL/min was used for each inducer.

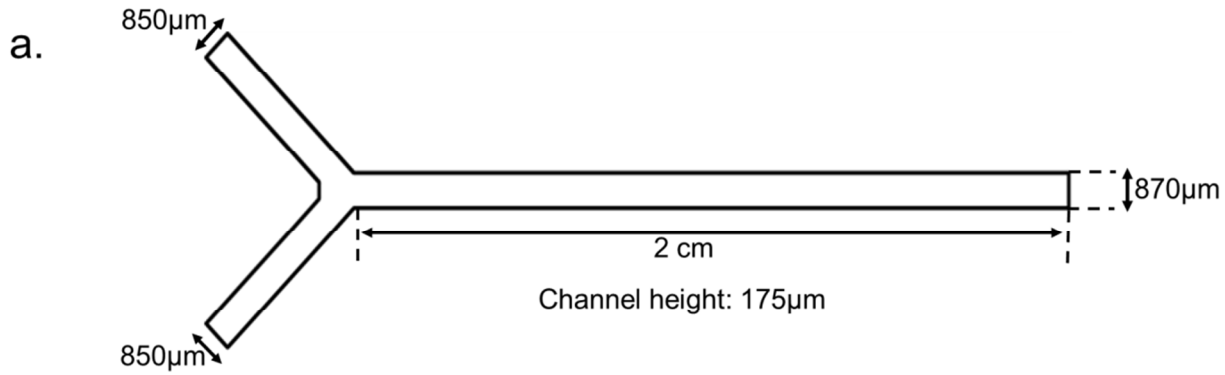

(*B*) Model-predicted IPTG inducer concentration profile. Inlet concentration is 1 mM.

(*C*) Model-predicted arabinose inducer concentration profile. Inlet concentration is 5 mM.

b.

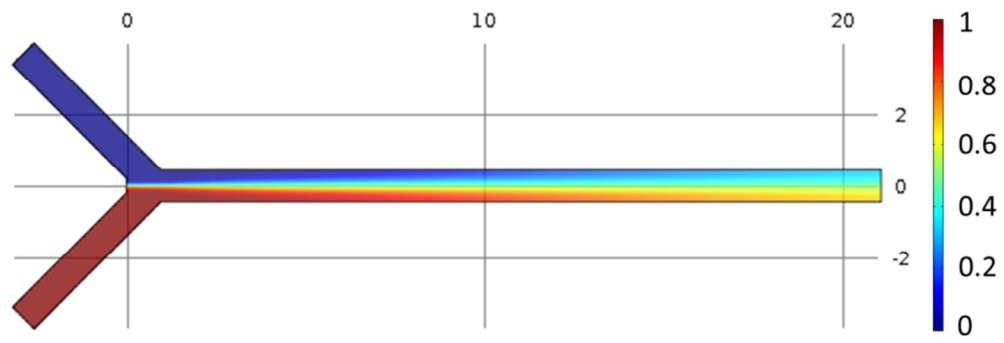

c.

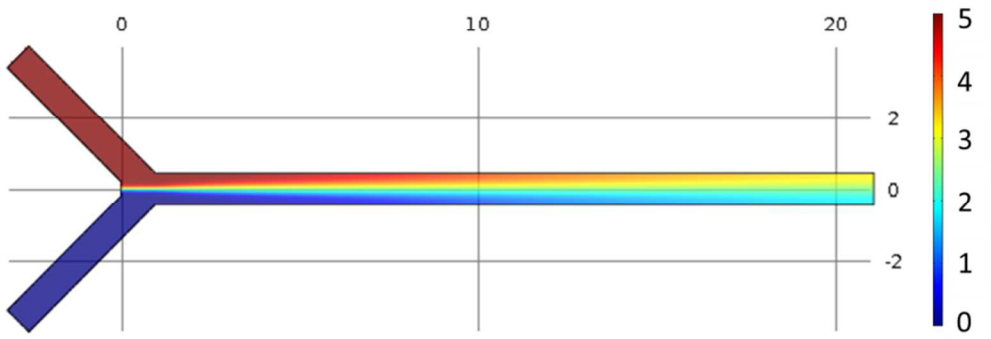

Figure S9. Model prediction and experimental measurement of dye diffusion in the microfluidic channel.

The diffusion of AlexaFluor488 dye in the microfluidic channel was computed under the conditions used for the experiments. Reported values for the diffusion coefficient of AlexaFluor488 dye range from 1.96 $\times 10^{-10}$ $m^2 \cdot s^{-1}$ to 4.62$\times 10^{-10}$ $m^2 \cdot s^{-1}$ at room temperature [14-20]. We used 4.3$\times 10^{-10}$ $m^2 \cdot s^{-1}$ because this value is commonly used[21-28] as the diffusion coefficient for this dye in water or aqueous buffer at room temperature. The diffusion profiles 0 mm, 6 mm and 12 mm downstream from the y-junction were predicted for AlexaFluor488. To verify these predictions, dye diffusion experiments were performed; the results closely matched the predicted concentration profiles. These results validated the prediction from simulations.

(*A*) To visualize diffusion in the laminar flow microfluidic channel, two liquid streams containing AlexaFluor488 dye (2.82 µM) and PBS were used. Fluorescence images were obtained from the glass-liquid interface inside the microfluidic channel. A series of images was obtained along the length of the channel and images were stitched together to provide the entire profile along the channel. Diffusion of dye at the interface of the two streams is visible along the length of the channel. (*B*) Diffusion of AlexaFluor488 dye in the microfluidic channel was modeled and the predicted profile of dye concentration at the liquid-surface interface along the entire length of the channel is plotted. AlexaFluor488 dye is depicted in red; PBS in blue.

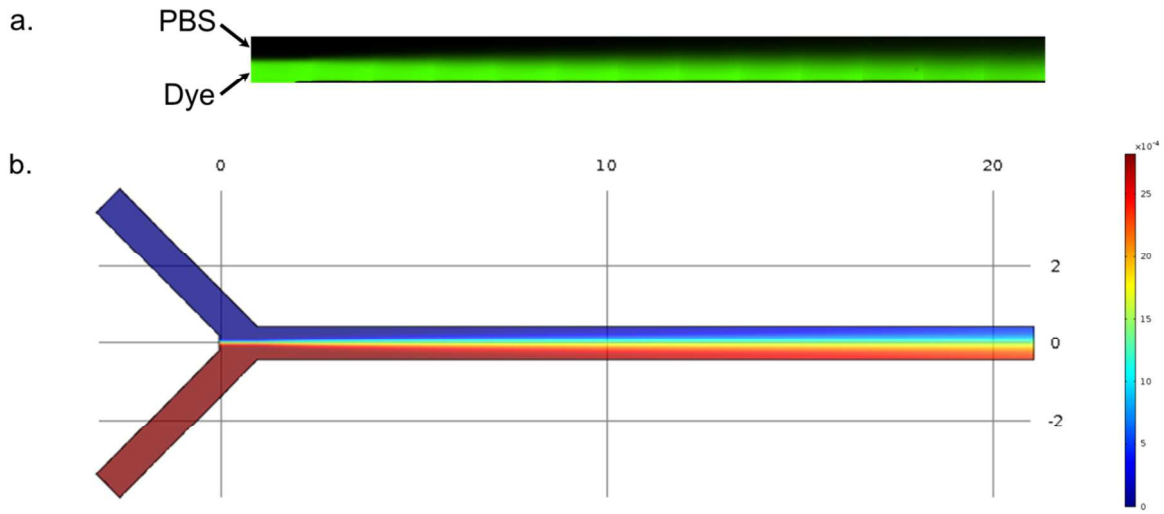

(**c**) Comparison of predicted and measured dye concentration profiles in the microfluidic channel. Predicted cross-channel dye profiles 0, 6, and 12 mm downstream from the y-junction are plotted as solid lines with color codes black, red and blue, respectively. Fluorescence quantification was also

performed at these locations. Experimental data points are plotted as open circles, color coded as above, and show good agreement between the predicted and measured dye concentration profiles.

C.

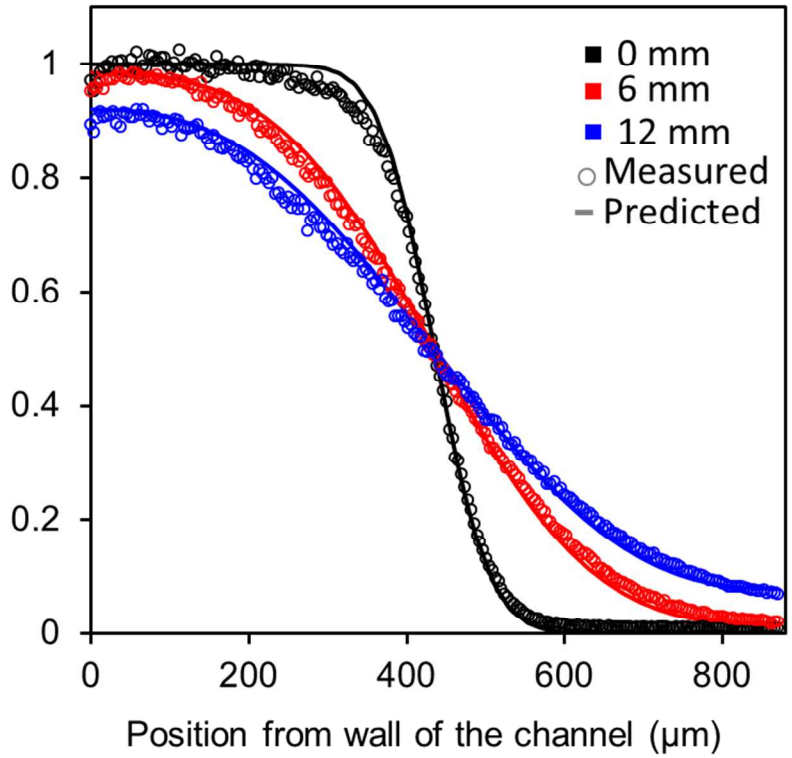

References:

(1) Segall-Shapiro, T. H.; Nguyen, P. Q.; Dos Santos, E. D.; Subedi, S.; Judd, J.; Suh, J.; Silberg, J. J. *J. Mol. Biol.* **2011**, *406*, 135.

(2) Somerville, C. R.; Ahmed, A. *J. Mol. Biol.* **1977**, *111*, 77.

(3) Hoff, K. G.; Culler, S. J.; Nguyen, P. Q.; McGuire, R. M.; Silberg, J. J.; Smolke, C. D. *Chem. Biol.* **2009**, *16*, 1299.

(4) Serre, L.; Verdon, G.; Choinowski, T.; Hervouet, N.; Risler, J. L.; Zelwer, C. *J. Mol. Biol.* **2001**, *306*, 863.

(5) Link, A. J.; Vink, M. K.; Tirrell, D. A. *Nat. Protoc.* **2007**, *2*, 1884.

(6) Hong, V.; Presolski, S. I.; Ma, C.; Finn, M. G. *Angew. Chem. Int. Ed.* **2009**, *48*, 9879.

(7) Anderson, J. R.; Chiu, D. T.; Jackman, R. J.; Cherniavskaya, O.; McDonald, J. C.; Wu, H.; Whitesides, S. H.; Whitesides, G. M. *Anal. Chem.* **2000**, *72*, 3158.

(8) Cowan, S. E.; Liepmann, D.; Keasling, J. D. *Biotechnol. Lett.* **2001**, *23*, 1235.

(9) Bashkatov, A. N.; Genina, E. A.; Sinichkin, Y. P.; Kochubey, V. I.; Lakodina, N. A.; Tuchin, V. V. *Biophys. J.* **2003**, *85*, 3310.

(10) Mogi, N.; Sugai, E.; Fuse, Y.; Funazukuri, T. *J. Chem. Eng. Data* **2007**, *52*, 40.

(11) Stewart, P. S. *J Bacteriol* **2003**, *185*, 1485.

(12) Nakanishi, K.; Ogiso, Y.; Nakama, T.; Fukai, S.; Nureki, O. *Nat. Struct. Mol. Biol.* **2005**, *12*, 931.

(13) Ngo, J. T.; Champion, J. A.; Mahdavi, A.; Tanrikulu, I. C.; Beatty, K. E.; Connor, R. E.; Yoo, T. H.; Dieterich, D. C.; Schuman, E. M.; Tirrell, D. A. *Nat. Chem. Biol.* **2009**, *5*, 715.

(14) Pristinski, D.; Kozlovskaya, V.; Sukhishvili, S. A. *J. Chem. Phys.* **2005**, *122*, 14907.

(15) Doeven, M. K.; Folgering, J. H.; Krasnikov, V.; Geertsma, E. R.; van den Bogaart, G.; Poolman, B. *Biophys. J.* **2005**, *88*, 1134.

(16) Modos, K.; Galantai, R.; Bardos-Nagy, I.; Wachsmuth, M.; Toth, K.; Fidy, J.; Langowski, J. *Eur. Biophys. J.* **2004**, *33*, 59.

(17) Needleman, D. J.; Xu, Y.; Mitchison, T. J. *Biophys. J.* **2009**, *96*, 5050.

(18) Ramadurai, S.; Duurkens, R.; Krasnikov, V. V.; Poolman, B. *Biophys. J.* **2010**, *99*, 1482.

(19) Sanchez, S. A.; Brunet, J. E.; Jameson, D. M.; Lagos, R.; Monasterio, O. *Protein Sci.* **2004**, *13*, 81.

(20) Vendelin, M.; Birkedal, R. *Am. J. Physiol. Cell Physiol.* **2008**, *295*, 24.

(21) Dross, N.; Spriet, C.; Zwerger, M.; Muller, G.; Waldeck, W.; Langowski, J. *PLoS One* **2009**, *4*, 4.

(22) Nitsche, J. M.; Chang, H. C.; Weber, P. A.; Nicholson, B. J. *Biophys. J.* **2004**, *86*, 2058.

(23) Oh, D.; Zidovska, A.; Xu, Y.; Needleman, D. J. *Biophys. J.* **2011**, *101*, 1546.

(24) Petrášek, Z.; Schwille, P. *Biophys. J.* **2008**, *94*, 1437.

(25) Ries, J.; Ruckstuhl, T.; Verdes, D.; Schwille, P. *Biophys. J.* **2008**, *94*, 221.

(26) Yordanov, S.; Best, A.; Weisshart, K.; Koynov, K. *Rev. Sci. Instrum.* **2011**, *82*, 036105.

(27) Zareh, S. K.; DeSantis, M. C.; Kessler, J. M.; Li, J. L.; Wang, Y. M. *Biophys. J.* **2012**, *102*, 1685.

(28) Zengel, P.; Nguyen-Hoang, A.; Schildhammer, C.; Zantl, R.; Kahl, V.; Horn, E. *BMC Cell Biol.* **2011**, *12*, 21.